PCCP

A spectroscopic study of the impact of pH and metal-to-ligand ratio on the speciation of the Pu(VI)-oxalate system

Journal:	*Physical Chemistry Chemical Physics*
Manuscript ID	CP-ART-08-2023-004010.R1
Article Type:	Paper
Date Submitted by the Author:	08-Nov-2023
Complete List of Authors:	Sockwell, Ashleigh; University of Notre Dame, Civil & Environmental Engineering & Earth Sciences DiBlasi, Nicole; University of Notre Dame, Civil & Environmental Engineering & Earth Sciences Hixon, Amy; University of Notre Dame, Civil & Environmental Engineering & Earth Sciences

A spectrophotometric study of the impact of pH and metal-to-ligand ratio on the speciation of the Pu(VI)-oxalate system

A. Kirstin Sockwell,[a]* Nicole A. DiBlasi,[a†] and Amy E. Hixon[a]

[a] Department of Civil & Environmental Engineering & Earth Sciences, University of Notre Dame, Notre Dame, IN 46556 USA

[†] Current address: Actinide Analytical Chemistry, Los Alamos National Laboratory, Los Alamos, NM 87545 USA

*corresponding author: asockwel@nd.edu

Abstract

The oxalate ligand is prevalent throughout the nuclear fuel cycle. While the Pu(III)- and Pu(IV)-oxalate systems are well studied due to their use in plutonium metal and PuO_2 production, the effect of oxalate on Pu(VI) remains understudied. Absorption spectroscopy was employed to probe the solution behavior of the Pu(VI)-oxalate system as a function of pH (1, 3, 7) and metal-to-ligand ratio (M/L; 10:1–1:10). Peak changes in the UV-vis-NIR spectra were associated with the formation of multiple Pu(VI)-oxalate species with increasing oxalate concentration. Some insight into identification of species present in solution was gained from the limited Pu(VI)-oxalate literature and comparisons with the assumed isostructural U(VI)-oxalate system. A peak in the UV-vis-NIR spectrum at 839 nm, which corresponds to the formation of a 1:1 $PuO_2(C_2O_4)(aq)$ complex, was observed and used to determine the formation constant ($\log \beta^\circ = 4.64 \pm 0.06$). A higher coordinated Pu(VI)-oxalate peak at 846 nm was tentatively assigned as the 1:2 complex $PuO_2(C_2O_4)_2^{2-}$ and a preliminary formation constant was determined ($\log \beta^\circ = 9.30 \pm 0.08$). The predominance of both complexes was shown in speciation diagrams calculated from the formation constants, illustrating the importance of considering the Pu(VI)-oxalate system in the nuclear fuel cycle.

1. Introduction

Oxalate ($C_2O_4^{2-}$) is an organic ligand that can be introduced into the nuclear fuel cycle during the reprocessing of spent nuclear fuel (SNF),[1] the preparation and purification of plutonium dioxide or plutonium metal,[2] as a byproduct of radiolytic degradation of intermediate-level nuclear wastes,[3] and through the decomposition of natural organic matter (NOM).[4,5] Due to multiple possible routes of oxalate introduction into the nuclear fuel cycle, there is a growing need to fully understand the impact of oxalate on the behavior of the actinide elements in chemical matrices that represent environmental and process systems. Specifically, expanding interest in the development and use of mixed-oxide (MOX) fuels, as well as ongoing environmental remediation and storage of legacy nuclear waste, necessitates a deeper understanding of the plutonium oxalate system.[6–8]

Extensive effort has been placed into the development of purification methods utilizing the relatively low solubility of tri- and tetravalent actinide oxalates in aqueous solutions. Precipitation of tetravalent Pu in the form of insoluble oxalates followed by calcination to form PuO_2(s) has been the industrial standard for purification of Pu for decades.[6,9–11] More recently, precipitation of trivalent Pu oxalate has been used as a path toward the preparation of suitable PuO_2(s) pellets for MOX fuels.[8,12] Early development of these precipitation methods has focused on increasing recovery efficiency and investigating the impact of various contaminants in the system on the recovery of Pu, rather than gaining new scientific understanding of the solution or solid-state chemistry. The quick reduction to primarily tetravalent Pu and subsequent precipitation has also led to a limitation of the oxidation states studied in the presence of oxalate. Thus, the mention of higher valence Pu oxalates in the literature is rare.

A further limitation in actinide oxalate literature arises from the emphasis on solid-state studies of actinide(IV) oxalates, as opposed to research aimed at describing the aqueous-phase

speciation of such systems. The low solubility of these oxalate compounds, along with the targeted approach toward this system for application rather than basic science, likely drove the literature toward this knowledge gap. Structural characterizations of some Pu-oxalate compounds have been published, but these studies are quite limited and primarily focus on the thermal degradation pathway from Pu(IV)-oxalate to PuO_2(s).[13,14] A larger collection of available uranium oxalate literature includes investigations pertaining to the U-oxalate system for U(IV) and U(VI) in both solid-state and aqueous systems. However, the aqueous studies are still significantly outnumbered by solid-state studies.

Only six articles on the aqueous Pu(VI)-oxalate system have been published and all have involved the use of spectrophotometric or potentiometric techniques.[1,4,15–18] Two aqueous Pu(VI)-oxalate complexes have been proposed—$PuO_2(C_2O_4)$(aq) and $[PuO_2(C_2O_4)_2]^{2-}$—but neither have been fully characterized.[16–18] In the solid-state, several possible Pu(VI)-oxalate compounds have been synthesized; again, limited characterization is available. Jenkins et al.[19] report powder X-ray diffraction data for hexavalent $PuO_2(C_2O_4)\cdot 3H_2O$(cr) and the isomorphous $UO_2(C_2O_4)\cdot 3H_2O$(s) compound.[19] Additionally, the electronic properties of the $PuO_2(C_2O_4)\cdot 3H_2O$(s) precipitate have been reported.[20,21] Bessonov et al.[20] propose electronic absorption peak assignments for $[PuO_2(C_2O_4)_2]^{2-}$ (837 nm), $PuO_2(C_2O_4)\cdot 3H_2O$(cr) (839 nm), $PuO_2(C_2O_4)\cdot H_2O$(cr) (844 nm), $(NH_4)_2(PuO_2)_2(C_2O_4)_3$(s) (845 nm), and $(NH_4)_2PuO_2(C_2O_4)_2$(s) (847 nm).[20] This group of compounds is assumed to share the pentagonal bipyramidal coordination of Pu(VI) present in the Pu(VI)-aquo ion due to the presence of a strong absorbance peak in the 830–850 nm region. An additional compound, $K_2(PuO_2)_2(C_2O_4)_3\cdot 4H_2O$(s), does not have a peak within this region and is assumed to provide an example of the hexagonal bipyramidal coordination of Pu(VI) and the resulting Laporte forbidden *f-f* transition.

U-oxalate and Np-oxalate studies may provide insight into the possible coordination of Pu(VI) in the presence of oxalate. According to analogous solid-state U(IV/VI) and Np(V) complexes, we expect Pu(VI) to coordinate with up to three oxalates, while lower oxidation states (e.g., Pu(IV)) may coordinate with up to five oxalates.[19,22–25] In the significantly larger library of U(VI)-oxalate structures, uranyl oxalate has been reported with two or three oxalates coordinated equatorially to the uranyl ion, resulting in a coordination number between 6 and 8.[24] When only two oxalates are coordinated to the uranyl ion, the equatorial plane is completed through coordination with a water molecule. In the aqueous system, 1:1, 1:2, 1:3, 2:3, and 2:5 U(VI)-oxalate complexes have all been proposed: $[(UO_2)(C_2O_4)(H_2O)]^-$, $[(UO_2)(C_2O_4)_2(H_2O)]^{2-}$, $(UO_2)(C_2O_4)_3(aq)$, $[(UO_2)_2(C_2O_4)_3]^{2-}$, and $[(UO_2)_2(C_2O_4)_5]^{6-}$, respectively. Several studies have determined that only the 1:1, 1:2, and 1:3 complexes were present under acidic conditions (pH < 1),[5,26,27] although it was unclear whether the third oxalate was coordinated in a monodentate or bidentate fashion. A spectrophotometric study of U(VI)-oxalate in 3 M $NaClO_4$ reports that all five complexes mentioned above were present and relevant to chemical modelling, but the 2:3 complex was a minor component with little contribution at pH 4.[28] The 2:5 complex has been identified in a UV-vis study in acetone.[29] Manfredi et al.[30] propose the existence of more than 10 equilibrium species in the ternary UO_2^{2+}-OH^--$C_2O_4^{2-}$ system when 4.5 < pH < 8.5. However, only three of the 10 proposed ternary complexes were identified by electrospray mass spectrometry: $[(UO_2)(OH)(C_2O_4)]^-$, $[(UO_2)_2(OH)_4(C_2O_4)_2]^{4-}$, and $[Na_4(UO_2)_2(OH)_2(C_2O_4)_4]^{2-}$.

The published literature shows that uncertainties remain regarding the aqueous–phase speciation of the U(VI)-oxalate system and thus, the extension of this speciation to the Pu(VI) system. This present study represents the first spectrophotometric investigation of the Pu(VI)-oxalate system as a function of pH (1, 3, 7) and metal to ligand ratio (M/L; 10:1–1:10). We used

UV-vis-NIR spectroscopy to investigate the formation of Pu(VI)-oxalate complexes in solution, providing insight into the behavior of Pu(VI) in the presence of oxalate. When possible, we identify specific species and calculate the respective formation constant.

2. Materials and Methods

CAUTION: Plutonium is radioactive and should only be handled by trained workers in approved facilities. These experiments were conducted in a specially designed laboratories licensed by the U.S. Nuclear Regulatory Commission and the University of Notre Dame Radiation Control Committee.

2.1 Materials

All chemicals were used as received. Oxalic acid dihydrate (98%) was purchased from Alfa-Aesar and sodium chloride (Certified ACS) was purchased from Fisher Scientific. Unless otherwise stated, MilliQ water (18.2 MΩ·cm at 25 °C) was used for dilutions.

2.2 Pu(VI) Stock Solution Preparation

A Pu(VI) working solution was prepared by oxidizing nominally weapon-grade Pu(VI) (>94% ^{239}Pu) in boiling concentrated nitric acid, followed by purification by column chromatography (Bio-Rad AG 1-X8 resin, 100-200 mesh) resulting in 3.445 ± 0.005 mM Pu(VI) in 3 M HNO_3. An aliquot of the stock (12 mL) was evaporated to dryness and the residue was dissolved in MilliQ water. The evaporation and dissolution processes were repeated at least three times before the final residue was dissolved in 0.1 M NaCl to yield a 19.574 ± 0.001 mM solution of Pu(VI). The Pu oxidation state was confirmed by UV-vis-NIR to be Pu(VI) (Figure S1) prior to the start of the experiments. A fresh working solution was created for each series of pH-specific experiments (pH = 1, 3, 7).

2.3 Experimental Setup and Analysis

All experimental solutions were prepared in a HEPA-filtered hood under ambient conditions. All pH measurements were performed with an Orion Star A211 pH meter (Thermo Scientific) coupled with a double junction semi-micro combination pH electrode (Orion, Thermo Scientific). A pH calibration was performed each day of use. All pH values are reported as experimental pH without ionic strength correction. The oxalate concentration was varied (0–10 mM) using 20 mM oxalate in 0.1 M NaCl. The pH of the oxalate stock was adjusted to 8.0 ± 0.5 with 0.1 M NaOH prior to use. Each vial was diluted to a total volume of 2 mL with 0.1 M NaCl, thus maintaining a constant ionic strength of 0.1 M for each experiment. The initial pH was adjusted to the target value (1, 3, 7) prior to Pu addition. Once the target pH was achieved, all solutions were spiked with the Pu(VI) working solution to result in an initial Pu concentration of 0.870 ± 0.006 mM. Experimental pH values were measured again prior to UV-vis-NIR analysis (Table S2) and were adjusted to the desired range, if necessary, with 0.1 M NaOH or 0.1 M HCl.

Samples were analyzed using a Cary 6000i UV-vis-NIR from 200–1200 nm with a scan rate of 60 nm·min^{-1} in a quartz cuvette with a 1-cm path length. A background subtraction was performed with 0.1 M NaCl. Each UV-vis-NIR spectrum was collected no more than 15 minutes after addition of Pu to the experimental solution. Molar extinction coefficients (ε) were calculated using the Beer-Lambert law[31,32] ($A = \varepsilon bC$). Uncertainties in molar extinction coefficients were calculated through error propagation using peak fitting procedure uncertainties (0.001–0.0001 A.U.) for absorbance and % RSD values for aqueous Pu concentrations that were determined via liquid scintillation counting (LSC).

2.4 Liquid scintillation counting (LSC)

Aqueous Pu concentrations were monitored by LSC on a PerkinElmer Tri-Carb 3110 TR liquid scintillation analyzer. Aliquots of experimental solutions (5 μL) were diluted into an organic LSC cocktail (4 mL, Wallack 'HiSafe') and measured for 5–60 minutes until appropriate counting statistics were achieved. Table S1 shows the aqueous Pu concentrations of each experimental solution following Pu spike into oxalate in 0.1 M NaCl.

3. Results

3.1 Ultraviolet-Visible-Near Infrared (UV-vis-NIR) Spectrophotometry

UV-vis-NIR spectrophotometry was used to study the speciation of the Pu(VI)-oxalate system as a function of pH (0.99 ± 0.08 (pH 1), 2.95 ± 0.35 (pH 3), and 6.94 ± 0.32 (pH 7)) and metal-to-ligand ratio (M/L; 10:1–1:10). These pH values were used to determine the effect of oxalate protonation (i.e., $H_2C_2O_4$, $HC_2O_4^-$, and $C_2O_4^{2-}$; (pKa(1)° = 4.250 ± 0.010; pKa(2)° = 1.400 ± 0.030))[33] on Pu(VI)-oxalate complex formation and Pu redox behavior. Experimental pH values are recorded in Table S2, Figure 1 shows absorption spectra of Pu(VI)-oxalate solutions at each investigated pH and M/L ratio, and Table 1 summarizes the major absorption peaks and proposed species assignments.

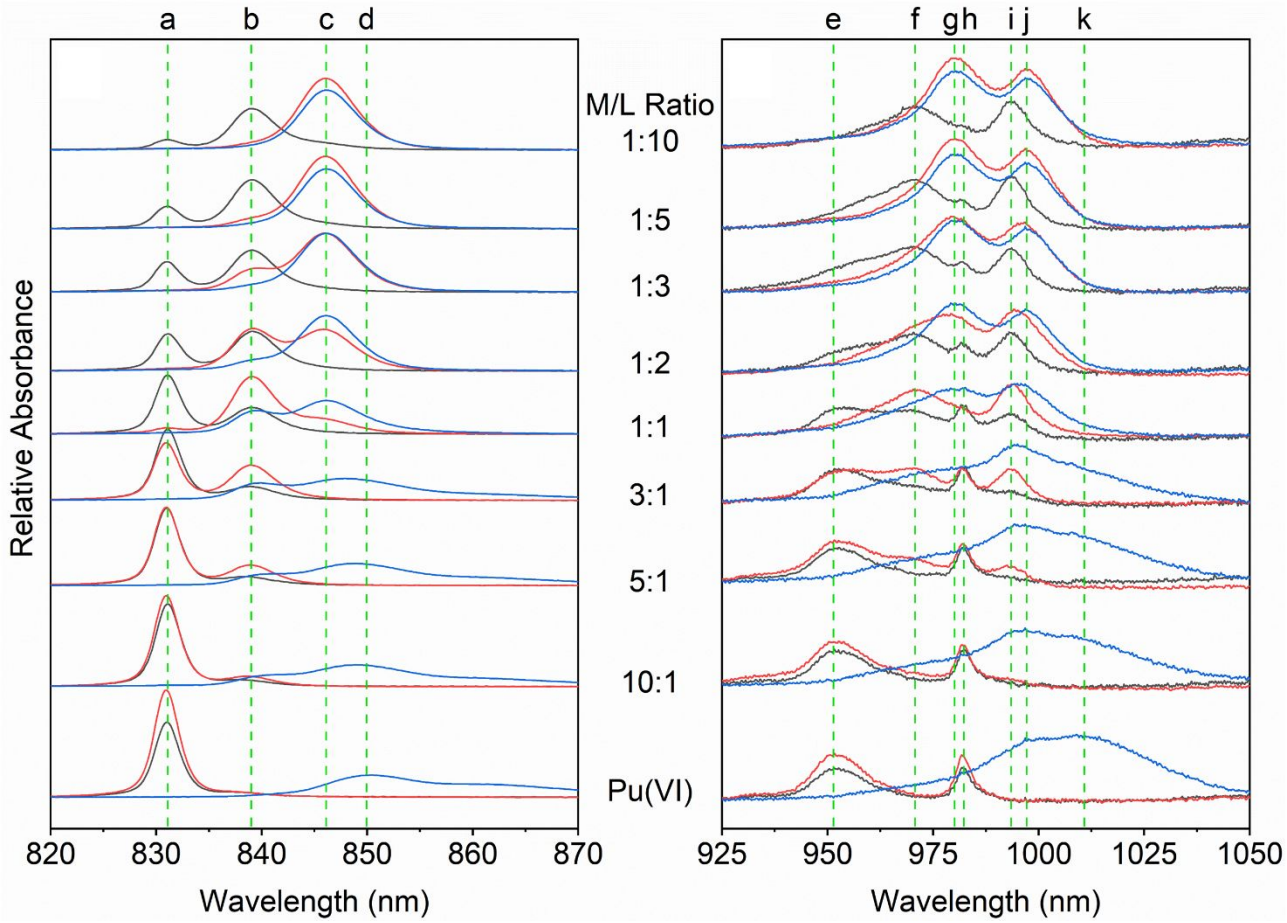

Figure 1. Comparison of UV-vis-NIR data from (left) 820–870 nm and (right) 925–1050 nm at pH 1 (black), pH 3 (red), and pH 7 (blue) as a function of metal-to-ligand (M/L) ratio (10:1–1:10). Samples were analyzed within 15 minutes of the Pu(VI) spike.

The spectra for Pu(VI) in the absence of oxalate show that no Pu reduction occurred at any investigated pH within the analysis time frame. The characteristic peaks representative of Pu(III), Pu(IV), and Pu(V) were not observed in the 200–700 nm region (Figure S2). In the mid-wavelength region (820–870 nm, Figure 1, left), the primary peak present at pH 1 was the characteristic Pu(VI)-aquo ion peak at 831 nm (peak a). An increase in the intensity of this peak was observed as the pH increased from 1 to 3. At pH 7, the peak became broader and exhibited a red shift that resulted in an absorption band with much smaller intensity centered at 850 nm (peak

d), which is indicative of Pu(VI) hydrolysis species.[34–36] Similar changes as a function of pH were observed in the higher wavelength range of the spectra (900–1050 nm, Figure 1, right). The Pu(VI)-aquo ion peaks at 952 and 982 nm (peaks e and h) were present at pH 1 and increased in intensity as the pH was raised from 1 to 3. At pH 7, these two peaks were no longer observed. Instead, a broad peak of higher intensity was observed from 975–1030 nm. Spectral deconvolution showed that this broad peak was best fit by two separate peaks centered at 997 and 1011 nm (peaks j and k), identified as Pu hydrolysis species within the literature.

For experiments containing Pu and oxalate at pH 1, new peaks were observed in both the mid- and high-wavelength ranges. A new peak at 839 nm (Figure 1, peak b) was observed after the addition of oxalate (M/L = 10:1). As shown in Figure 2a, the intensity of the 839 nm peak increased with increasing oxalate concentration ([L]), whereas the intensity of the PuO_2^{2+} peak at 831 nm decreased with increasing [L]. Both peaks were present even at the highest oxalate concentration (M/L = 1:10). In the high-wavelength region (Figure 1, right), new peaks at 971 and 993 nm (peaks f and i) were observed when M/L = 1:1. In the presence of excess oxalate ([M] ≤ [L]), the intensity of these new peaks increased with oxalate concentration and the intensity of the PuO_2^{2+} peaks at 952 and 982 nm decreased with increasing [L]. Unlike in the mid-wavelength region, the PuO_2^{2+} peaks were not present at M/L = 1:10.

In solutions containing Pu and oxalate at pH 3, a similar growth of new peaks coupled with the loss of peaks associated with the Pu(VI) aquo ion was observed as oxalate concentrations were increased. The 839 nm peak appeared when M/L = 10:1 and the complete loss of the PuO_2^{2+} peak at 831 nm occurred in the presence of equimolar oxalate (M/L = 1:1). A second peak was observed at 846 nm (Figure 1, peak c) when [M] ≤ [L] and gained intensity as the intensity of the 839 nm peak decreased; the 839-nm peak was no longer apparent when M/L = 1:10 (Figure 2b). In the

high-wavelength region, the PuO_2^{2+} peaks were not present when [M] ≤ [L]. The 971 and 993 nm peaks appeared when M/L = 5:1 and increased with increasing [L] until M/L = 1:1. When oxalate was in excess, the 971 and 993 nm peaks exhibited a red-shift with increasing [L]. The final peak positions were 979 and 997 nm (Figure 1, peaks g and j), respectively, at M/L = 1:10 (Figure S3b).

In the mid-wavelength region at pH 7, both the 839 and 846 nm peaks were observed in the presence of oxalate. The 846 nm peak resulted from a blue-shift of the Pu(VI) hydrolysis peak (850 nm) over the range M/L = 10:1–1:1 and slightly increased in intensity at higher [L] (Figure 2c). The 839 nm peak only appeared when [M] ≥ [L] and remained a minor peak compared to those at 850 nm and 846 nm. In the high-wavelength region of the UV-vis-NIR spectrum, the Pu(VI) hydrolysis peak at 997 nm persisted across the entire range of M/L ratios. Instead, changes were observed in the Pu(VI) hydrolysis peak at 1011 nm, which decreased in intensity with increasing [L]. When [M] ≤ [L], peak in growth was observed at 979 nm (Figure S3c).

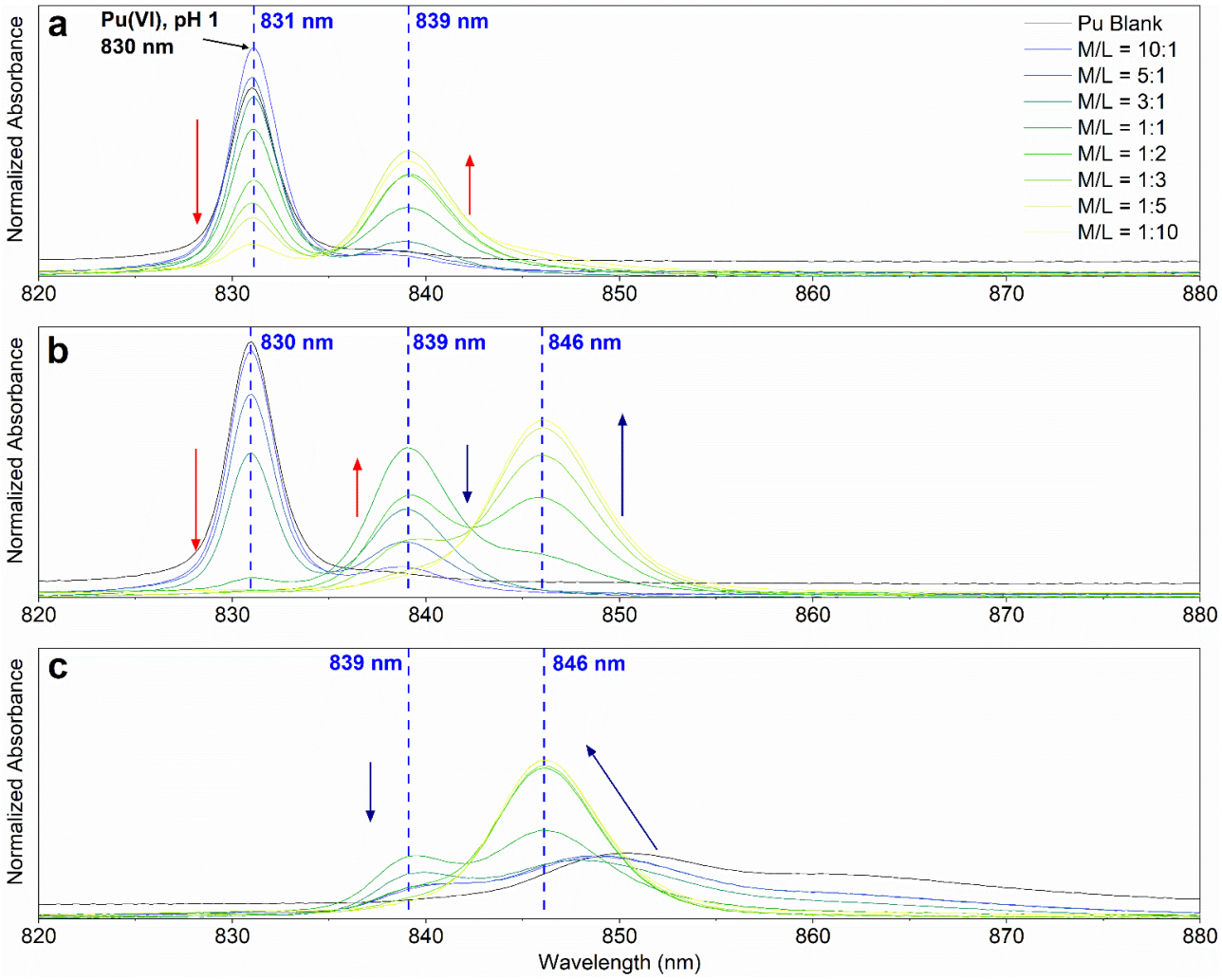

Figure 2. UV-vis-NIR spectra of Pu(VI)-oxalate experiments at (a) pH 1, (b) pH 3, and (c) pH 7 from 820–880 nm. Red and blue arrows show changes in peak intensity or shifts in peak position with increasing [L].

4. Discussion

4.1 UV-vis-NIR Spectroscopy

Samples containing only Pu(VI) and 0.1 M NaCl were analyzed with absorption spectrophotometry to monitor the initial oxidation state present at each experimental pH (1, 3, 7). The presence of the characteristic Pu(VI) peaks and lack of Pu(V) and Pu(IV) peaks indicated that,

at t < 15 minutes in the absence of oxalate, Pu was present only as the +VI oxidation state in solution.[1] At pH 1 and 3, only the intense peak at 831 nm, indicative of PuO_2^{2+}, was present between 800 and 900 nm. At pH 7, broad peaks centered at 850 nm and 1011 nm represented the formation of Pu(VI)-hydrolysis complex(es) in solution (Figure S4). Thermodynamic calculations were performed to better predict the species present in each system (see Section 4.3). The resulting speciation diagrams (Figure S5) show that the predicted dominant species of Pu(VI) in the absence of oxalate is PuO_2^{2+} at pH 1 and 3 and $[PuO_2OH]^+$ or $[(PuO_2)_2(OH)_2]^{2+}$ at pH 7 in the presence of atmospheric carbonate.[1,35,37,38]

Changes in the sharp, strong 831 nm peak representative of the Pu(VI) *f-f* transition were used to monitor the loss of the Pu(VI)-aquo ion with increasing [L]. Only one spectroscopic study of the Pu(VI)-oxalate system has been reported,[20] so additional guidance for understanding changes in our systems was obtained from previous reports on the spectral impact of changing Pu(VI) coordination.[39–45]

Table 1: Proposed UV-vis-NIR peak assignments for the Pu(VI)-oxalate system.[1,46] Peak ID refers to the vertical, green, dashed lines in Figure 1.

Peak ID	Peak (nm)	Proposed Species Assignment	Reference
a	831	PuO_2^{2+}	1
b	839	$PuO_2(C_2O_4)(aq)$	This work
c	846	$[PuO_2(C_2O_4)_2]^{2-}$	This work
d	850	$[PuO_2OH]^+$ or $[(PuO_2)_2(OH)_2]^{2+}$	1,35,37
e	952	PuO_2^{2+}	1
f	971	$PuO_2(C_2O_4)(aq)$	This work
g	979	$[PuO_2(C_2O_4)_2]^{2-}$	This work
h	982	PuO_2^{2+}	1
i	993	$PuO_2(C_2O_4)(aq)$	This work
j	997	$[(PuO_2)_m(OH)_n]^{(2m-n)+}$ $[PuO_2(C_2O_4)_2]^{2-}$	46 This work
k	1011	$[(PuO_2)_m(OH)_n]^{(2m-n)+}$	46

The peaks at 839 and 846 nm were determined to represent Pu(VI)-oxalate complexes that shared the pentagonal bipyramidal coordination environment of the fully hydrated Pu(VI)-aquo ion ($[PuO_2(H_2O)_6]^{2+}$).[47] The strong peaks in the 830–850 nm region were lost as the *f-f* transition became Laporte forbidden with the addition of an inversion center (i.e., hexagonal bipyramidal coordination).[20] A similar loss of peaks in the 830–850 nm region with changing Pu(VI) coordination geometry has previously been reported.[44,45] By assuming that the presence of peaks within the 830–850 nm region are dependent on the presence of Pu(VI) in hexagonal bipyramidal coordination, the identification of species correlating to the new peaks observed in the current work may be proposed. The presence of two peaks at 839 and 846 nm, which have distinct growth trends with the addition of oxalate, suggests the formation of at least two Pu(VI) oxalate species in solution. The 839 nm peak, which was predominantly observed at pH 1 and 3, is consistent with the previously-observed peak corresponding to the 1:1 $PuO_2(C_2O_4)\cdot 3H_2O(s)$ compound, while the 846 nm peak observed at pH 3 and 7 was similar to the peak previously identified for the solid 2:3

and 1:2 compounds $(NH_4)_2(PuO_2)_2(C_2O_4)_3$(s) (845 nm) and $(NH_4)_2PuO_2(C_2O_4)_2$(s) (847 nm), respectively.[20] Therefore, we assign the 839 nm peak to $PuO_2(C_2O_4)$(aq) and the 846 nm peak to species like $[PuO_2(C_2O_4)_2]^{2-}$ and/or $[(PuO_2)_2(C_2O_4)_3]^{2-}$.

Although the comparison of aqueous and solid-state absorption data is not ideal, the limited nature of the literature has necessitated this comparison. Additional support for our conclusions can be drawn from similar systems in the literature. Pu(VI) coordination with chloride[40–42] and carboxylate ligands such as dipicolinic acid (DPA),[44] iminodiacetic acid (IDA),[45] and methyliminodiacetic acid (MIDA)[45] has been reported to form 1:1 species with absorption peaks between 838 and 841 nm and 1:2 species with peaks between 843 and 852 nm. For example, the 1:1 species PuO_2(DPA)(aq) and $PuO_2(IDA)(H_2O)_3$(aq) have strong absorption peaks at 838 and 840.6 nm, respectively.[44,45] Direct comparison of the 846 nm peak is more difficult due to the observed impact of the complexing ligand on the precise location and shape of this peak. Given that the 1:2 species $[PuO_2(IDA)_2]^{2-}$ has strong absorption at 853.3 nm,[45] we propose that the 846 nm peak is indicative of the 1:2 species $[PuO_2(C_2O_4)_2]^{2-}$.[16–18,20]

Little attention has been focused on the importance of the high-wavelength region (900–1050 nm) in the literature. The current work has monitored similar changes in this region as noted in the mid-wavelength region (820–870 nm), further supporting the formation of multiple Pu(VI) oxalate complexes in solution with the addition of oxalate. At pH 1 and 3, the loss of intensity of the Pu(VI)-aquo ion peaks (952 and 982 nm) were nearly mirrored by the intensity loss of the 831 nm peak. Slight differences of intensity loss between the regions are likely due to the lower molar absorptivity of the high-wavelength peaks compared to the mid-wavelength region. Similarly, the Pu(VI)-hydrolysis complex peaks (997 and 1011 nm) lost intensity in a comparable manner as the 850 nm peak, where increasing [L] led to a decrease of Pu(VI)-hydrolysis peaks. The oxalate-

dependent peaks in the high-wavelength region may be paired with peaks in the mid-wavelength region and the corresponding Pu(VI)-oxalate complexes. The 971 and 993 nm peaks increase in intensity similar to the 839 nm peak, and thus can be assigned to the 1:1 species $PuO_2(C_2O_4)(aq)$. The 979 and 997 nm peaks behave the same as the 846 nm peak, and thus are assigned as $[PuO_2(C_2O_4)_2]^{2-}$.

4.1.1 Impact of pH

Varying the pH of experimental solutions can impact the hydrolysis of Pu(VI) and protonation state of the oxalate. A change in the speciation of Pu(VI) in the absence of oxalate was only observed for samples at pH 7, as displayed by the shift in the 831 nm peak to higher wavelength (850 nm). This shift is consistent with hydrolysis of the Pu(VI)-aquo ion.[1] Thermodynamic calculations show the presence of two possible hydrolysis species at this pH: $[PuO_2OH]^+$ and $[(PuO_2)(OH)_2]^{2+}$ (Figure S5).

The pH displayed an impact on the formation of Pu(VI)-oxalate complexes in solution. At pH 1, the oxalate is expected to be fully protonated (i.e., $H_2C_2O_4(aq)$, Figure S5), and thus less likely to fully coordinate with available metals. The continued presence of the Pu(VI) peak at 831 nm with an excess of oxalate, likely due to the lack of coordination with the fully protonated oxalate, agrees with this assumption. However, the appearance of the 839 nm peak, identified as a 1:1 Pu(VI) oxalate complex, indicates that, even though the free oxalate is fully protonated and complete complexation of all available Pu did not occur, limited complexation reactions still proceeded under these conditions.

At higher pH, partial ($HC_2O_4^-$, pH 3) or full ($C_2O_4^{2-}$, pH 7) deprotonation of oxalate (Figure S5) is expected to lead to more complexation with available metals than at lower pH because of the availability of bonding sites and a negative charge on the free ligand, which would result in

stronger interactions with the positively charged Pu(VI) ions in solution.[33] The complete loss of the characteristic Pu(VI) peak at pH 3 (831 nm) and pH 7 (850 nm) with increasing [L] suggests a loss of the Pu(VI)-aquo ion and Pu(VI) hydrolysis products, respectively. Distinct peaks at 839 and 846 nm were observed at both pH 3 and 7, indicating the presence of two Pu(VI)-oxalate complexes in solution. The 1:1 complex formed in a lower concentration at pH 7 than in the pH 3 system, as seen by the overall lower intensity of the 839 nm peak and its subsequent decrease in intensity with increasing [L]. Figure S5 shows the loss of PuO_2^{2+} with the growth of the 1:1 complex, agreeing with the observations in the absorption data. Although ternary complexes have been reported for the U(VI)-oxalate system (i.e., $[(UO_2)(OH)(C_2O_4)]^-$, $[(UO_2)_2(OH)_4(C_2O_4)_2]^{4-}$, and $[Na_4(UO_2)_2(OH)_2(C_2O_4)_4]^{2-}$),[30] evidence of similar Pu species was not observed. The spectroscopic similarities of the pH 3 and pH 7 systems in the presence of excess oxalate suggest the presence of similar species. As the ternary hydrolysis complexes would not be expected at pH 3, the data does not provide sufficient evidence toward the presence of these species at pH 7.

4.1.2 Impact of Metal to Ligand (M/L) Ratio

At pH 1 and 3, we observed a decrease in the Pu(VI)-aquo ion peak at 831 nm with [L] accompanied by the growth of Pu(VI)-oxalate coordination peaks at 839 and 846 nm, suggesting the formation of multiple coordination complexes with changing M/L ratio. The 839 nm peak was observed with just 0.1 equivalents of oxalate in the presence of Pu(VI) at all three investigated pHs, indicating favorable coordination of Pu(VI) by oxalate under the experimental conditions investigated within this study. With increasing [L], the Pu(VI)-aquo ion peaks (831, 952, and 982 nm) either decreased in intensity (pH 1) or were completely lost (pH 3 and 7) and were replaced by peaks indicative of Pu(VI)-oxalate complex formation (839 and 846 nm).

While all three investigated pHs displayed clear isosbestic points with increasing [L] (Figure 2), the spectral changes for the pH 3 experiments were the most dynamic with changing M/L (Figure 2b). Between M/L = 3:1 and M/L = 1:1, the first isosbestic point at ~835 nm formed as the peak representative of PuO_2^{2+} (831 nm) was completely replaced by the peak assigned as the $PuO_2(C_2O_4)(aq)$ complex (839 nm). At M/L = 1:1, the spectrum suggested that nearly all Pu(VI) was coordinated, providing further support that the 839 nm peak represents the 1:1 Pu(VI)-oxalate aqueous complex. A second isosbestic point between the 839 and 846 nm peaks was observed when [M] ≤ [L], indicating a clear mixture of two separate Pu-oxalate complexes in solution upon complete complexation. As [L] was increased so that M/L = 1:2, the 839 and 846 nm peaks became nearly equivalent in intensity. Increasing the [L] further pushed the second isosbestic point towards the higher wavelength peak, resulting in the complete replacement of the 839 nm peak with the 846 nm peak in the presence of an excess of oxalate. The loss of the 839 nm peak in the presence of excess oxalate agrees with the assignment of the 839 nm peak as the 1:1 Pu(IV)-oxalate complex. We have tentatively assigned the 846 nm peak to the 1:2 Pu(VI)-oxalate complex $[PuO_2(C_2O_4)_2]^{2-}$, but further work is necessary to definitively confirm this peak assignment due to the overall complexity of the system and the predominance of multiple equilibrium complexes in solution simultaneously. The relative intensities of the two aqueous complexation peaks were equivalent at M/L = 1:2 and only a slight increase in intensity was observed for the 846 nm peak when [M] ≤ 3[L] after the loss of the 839 nm peak. Due to the likely equilibrium between the 1:1 and 1:2 Pu(VI)-oxalate species, we believe this increase is due to the completion of the replacement of 1:1 species with the 1:2 species, and not a higher coordination complex.

The experiments conducted at pH 1 and 7 exhibited similar trends, but with only one observed isosbestic point instead of two. At pH 1, increasing [L] led to a near complete loss of the 831 nm peak and the formation of the 1:1 Pu(VI)-oxalate complex, as indicated by the presence of only the 839 nm peak at equimolar and higher ligand concentrations (Figure 2a). At pH 7, the 839 nm peak representative of the 1:1 Pu(IV)-oxalate complex was present, but not favored (Figure 2c). Instead, the 846 nm peak grew in and dwarfed the lower wavelength 839 nm peak, thus suggesting the favorable formation of complexes with more coordinated ligands (i.e., $[PuO_2(C_2O_4)_2]^{2-}$) than observed at lower pH. This agrees with the expectation that higher coordination is favored under conditions which promote ligand deprotonation, such as higher pH, due to the availability of more free coordination sites on the ligand.

4.3 Molar Absorption Coefficient and Thermodynamic Calculations

UV-vis-NIR results were coupled with total aqueous Pu concentrations from liquid scintillation counting analyses to calculate molar extinction coefficients (ε) for the Pu(VI)-aquo ion and Pu(VI)-oxalate complex peaks identified in the mid-wavelength range (820–870 nm) of pH 3 solutions (Table 2). In the pH 3 system, the 830 and 846 nm peaks were isolated and peak fit. The peak data, along with [Pu] from LSC allowed for the calculation of the ε value for each peak. From these values, the ε value for the 839 nm peak was calculated. The ε value for the Pu(VI) spectra in the absence of oxalate at pH 3 was significantly lower than the published literature value (555 $cm^{-1}M^{-1}$).[1] This discrepancy can be attributed to spectral changes that occur with increasing pH, as the literature value was collected for a solution at pH 0. In fact, Figure 1 displayed a lower absorption intensity at ~830 nm for the Pu(VI) solution in the absence of oxalate at pH 3 when compared to the spectrum collected at pH 1, providing further support for a lower calculated ε value at elevated pH. This result thus provided verification of methodology and the calculations

performed for all other identified peaks within the UV-vis-NIR spectra. In the absence of oxalate, only one peak was observed in the mid-wavelength region, which was attributed to the Pu(VI) aquo ion. For this reason, calculations were performed assuming no contributions from chloride or hydrolysis species.

Table 2. Calculated molar extinction coefficients for selected peaks identified within absorption spectra of pH 3 solutions with M/L = 1:0 to 1:10.

Experiment	Absorption Maxima (nm)	Calculated ε (cm^{-1} M^{-1})	Assigned Aqueous Speciation
Pu(VI) Control (no oxalate), pH 3	830	356 ± 36	$[PuO_2(H_2O)]^{2+}$
Pu(VI)-Oxalate, pH 3	831	362 ± 70	$[PuO_2(H_2O)]^{2+}$
	839	311 ± 62	1:1 complex, $PuO_2(C_2O_4)(aq)$
	846	243 ± 24	$[PuO_2(C_2O_4)_2]^{2-}$

Following the determination of ε values, we were able to calculate the ionic strength corrected formation constant for the 1:1 Pu(VI)-oxalate complex, $PuO_2(C_2O_4)(aq)$, at pH 3 according to reaction 1.

$$PuO_2^{2+} + HC_2O_4^- \leftrightarrow PuO_2(C_2O_4)(aq) + H^+ \qquad \log K° = 0.39 \pm 0.06 \qquad (1)$$

Thermodynamic calculations were performed using the Medusa/Spana software package[48] to verify the speciation of both oxalate and Pu(VI) as a function of pH prior to complexation under the appropriate experimental conditions (Figure S5). From these calculations, we determined that oxalate would be predominately singly protonated, and Pu(VI) would be found as the PuO_2^{2+}

cation in solution prior to solution mixing at pH 3 and in the presence of atmospheric carbon dioxide.

The formation constant for the 1:1 species was then used to determine a preliminary formation constant for the 1:2 species $[PuO_2(C_2O_4)]^{2-}$ identified at 846 nm using the isosbestic point (i.e., equilibrium) observed between the 1:1 and 1:2 species (reaction 2):

$$PuO_2(C_2O_4)(aq) + HC_2O_4^- \leftrightarrow [PuO_2(C_2O_4)]^{2-} + H^+ \qquad \log K° = 0.41 \pm 0.05 \qquad (2)$$

For further thermodynamic calculations, protonation constants for oxalate were taken from Hummel et al.,[33] free proton concentrations were calculated based off the experimentally measured pH values (Table S2), and ionic strength was corrected for using the Specific Ion-interaction Theory (SIT) activity model (Table S5).[49] The resulting formation constants for the $PuO_2(C_2O_4)(aq)$ and $[PuO_2(C_2O_4)]^{2-}$ species were further applied to the speciation calculations, and evidence of their predominance in solution from pH 2–8 is highlighted within the speciation diagrams shown in Figure S5.

By correcting reactions 1 and 2 to consider the protonation constants of oxalate to achieve the simplest reaction between the free Pu(VI)-aquo ion and the fully deprotonated oxalate, we were able to calculate a second apparent formation constant for both $PuO_2(C_2O_4)(aq)$ and $PuO_2(C_2O_4)^{2-}$ (reactions 3–4), which are better equipped for comparison to literature values (reactions 5–6).

$$PuO_2^{2+} + C_2O_4^{2-} \leftrightarrow PuO_2(C_2O_4)(aq) \qquad \log \beta° = 4.64 \pm 0.06 \qquad (3)$$

$$PuO_2^{2+} + 2C_2O_4^{2-} \leftrightarrow [PuO_2(C_2O_4)_2]^{2-} \qquad \log \beta° = 9.30 \pm 0.08 \qquad (4)$$

$UO_2^{2+} + C_2O_4^{2-} \leftrightarrow UO_2(C_2O_4)(aq)$ $\log \beta° = 7.13 \pm 0.16$ (5)[33]

$UO_2^{2+} + 2C_2O_4^{2-} \leftrightarrow [UO_2(C_2O_4)_2]^{2-}$ $\log \beta° = 11.65 \pm 0.15$ (6)[33]

The comprehensive review published by Hummel et al.[33] discusses formation constants of additional radionuclide-oxalate complexes in detail, thus providing a repository of available literature values to compare with the constant generated within this work. Hummel et al.[33] lists only one apparent formation constant for the $PuO_2(C_2O_4)(aq)$ species ($\log \beta = 6.64$), which was determined by Gel'man et al.[15] through a low pH solubility study at $I = 1$ M HNO_3. This study resulted in an approximate formation constant for the $[PuO_2(C_2O_4)_2]^{2-}$ species ($\log \beta = 11.5$). The review also discusses a second apparent formation constant for $[PuO_2(C_2O_4)_2]^{2-}$ ($\log \beta = 9.35 \pm 0.5$), determined through a well-controlled potentiometric study ($I = 1.0$ M). None of the aforementioned values were corrected for ionic strength effects and they have not been verified in any additional studies. Ultimately, these values were not selected for inclusion in the NEA-TDB due to the typical instability of Pu(VI) in oxalate solutions, the uncertainties concerning the accuracy of the solubility data, and the lack of additional research supporting the thermodynamic values for the 1:1 species.[33]

In contrast, the NEA-TDB lists 31 separate apparent and absolute formation constant values for the U(VI) analog of the 1:1 oxalate complex, which range from 3.22 to 7.37, depending on the experimental conditions, and 21 separate apparent and absolute formation constant values for the U(VI) analog of the 1:2 oxalate complex, ranging from 6.47 to 14.08. Through a series of strict selection criteria, Hummel et al.[33] selected a single reliable value ($\log \beta° = 7.13 \pm 0.16$) for the formation of the analogous 1:1 U(VI)-oxalate complex (reaction 5) and a single reliable value

(log $\beta°$ = 11.65 ± 0.15) for the formation of the analogous 1:2 U(VI)-oxalate complex (reaction 6).[33]

Both the proposed Pu values by Gel'man et al.[16] and Portanova et al.[17] and the NEA-TDB selected U values are similar to the value for the $PuO_2(C_2O_4)(aq)$ and $[PuO_2(C_2O_4)]^{2-}$ complexes calculated in the present work, and the difference between the 1:1 and 1:2 formation constants is ~5 log units for both the literature U values and our calculated Pu values. This provides further support for the reliability of these calculations. Additionally, the calculated values for the 1:1 Pu(VI)-oxalate complex falls near the middle of the range of values provided within the NEA-TDB review for all analogous U complexes. As Hummel et al.[33] did not select any Pu-oxalate complexes within their review, and the only listed values were not corrected for ionic strength, further direct comparison of Pu to U values for the oxalate is not reasonable. However, additional spectrophotometric, potentiometric, calorimetric, and capillary electrophoresis ICP-MS studies of the U(VI)-oxalate system were published after the NEA-TDB review.[50–53] These studies provide a smaller range of values for the absolute formation constant of the $UO_2(C_2O_4)(aq)$ complex (i.e., log $\beta°$ = 6.96–7.71) and the absolute formation constant for the $[UO_2(C_2O_4)_2]^{2-}$ complex (i.e., log $\beta°$ = 11.45–12.07). The most notable observation of these more recent studies is the comparison of stability constants across the actinide series conducted by Brunel et al.,[53] who discuss stability constants obtained through capillary electrophoresis techniques at 25 °C and extrapolated to zero ionic strength by SIT for U(VI), Np(V), Pu(V), and Am(III). While it is not reasonable to directly compare formation constants for aqueous complexes with different metal oxidation states, a trend was still observed when comparing Np(V) and Pu(V) values: formation constants for analogous complexes decreased across the actinide series. From this, we would expect the Pu(VI)-oxalate formation constants to be smaller in magnitude than the U(VI)-oxalate formation constants, which

agrees with the comparison provided in reactions 3–6. This observation, along with the similarities between the Pu values generated within this work and the U values selected by the NEA-TDB, provides further support for our assignment of the 1:1 and 1:2 Pu(VI)-oxalate complexes, $PuO_2(C_2O_4)(aq)$ and $[PuO_2(C_2O_4)_2]^{2-}$, to the initial peaks observed within the UV-vis-NIR spectra from M/L = 1:0 to 1:10 at pH 3, thus partially clarifying the as yet undefined speciation within the Pu(VI)-oxalate system.

5. Conclusions

In this work, we have presented the first spectrophotometric study of the aqueous Pu(VI)-oxalate system. UV-vis-NIR spectroscopy was used to investigate the system as a function of pH (1, 3, 7) and M/L (10:1 to 1:10). Several new peaks in the UV-vis-NIR spectra were observed with increasing oxalate concentration. These peaks were determined to represent the presence of multiple Pu(VI)-oxalacte species in solution. We have assigned the 1:1 Pu(VI)-oxalate complex, $PuO_2(C_2O_4)(aq)$, to a peak at 839 nm and tentatively identified the 1:2 complex, $PuO_2(C_2O_4)_2^{2-}$ as responsible for the peak at 846 nm. The absolute formation constant of the 1:1 complex was determined ($\log \beta^\circ = 4.64 \pm 0.06$). Due to the complexity of the system, only a preliminary formation constant was determined for the 1:2 complex ($\log \beta^\circ = 9.30 \pm 0.08$). Both values were within reasonable agreement with the literature concerning $UO_2(C_2O_4)(aq)$ and $[UO_2(C_2O_4)_2]^{2-}$, further supporting our assignments.

Acknowledgements

This material is based upon work supported by the Department of Energy (DOE), Office of Basic Energy Sciences (SC), Heavy Element Chemistry Program under Award Number DE-SC0018231. N. A. DiBlasi was supported by an appointment to the DOE Scholars Program,

sponsored by the DOE, administered by the Oak Ridge Institute for Science and Education, and funded by the WIPP Project (DOE-CBFO).

Declaration of Competing Interest

The authors declare that they have no known competing financial interests or personal relationships that could have appeared to influence the work reported in this paper.

References

1 M. Altmaier, X. Gaona, D. Fellhauer, D. L. Clark, W. H. Runde and D. E. Hobart, in *Plutonium Handbook*, eds. D. L. Clark, D. A. Geeson and R. J. Hanrahan Jr, American Nuclear Society, 2nd edn., 2019, vol. 3, pp. 1543–1726.

2 J. F. Facer Jr. and K. M. Harmon, *Precipitation of Plutonium(IV) Oxalate. HW-31186*, Richland, WA, USA, 1954.

3 A. Bertron, N. Jacquemet, B. Erable, C. Sablayrolles, G. Escadeillas and A. Albrecht, *Nucl. Eng. Des.*, 2014, **268**, 51–57.

4 D. T. Reed, D. G. Wygmans, S. B. Aase and J. E. Banaszak, *Radiochim. Acta*, 1998, **82**, 109–114.

5 D. Ferri, M. Iuliano, C. Manfredi, E. Vasca, T. Caruso, M. Clémente and C. Fontanella, *J. Chem. Soc., Dalton Trans.*, 2000, **4**, 3460–3466.

6 C. A. Nash, *Literature Review for Oxalate Oxidation Processes and Plutonium Oxalate Solubility. SRNL-STI-2012-00003*, Savannah River National Laboratory, Aiken, SC, USA, 2012.

7 J. F. Corbey, L. E. Sweet, S. I. Sinkov, D. D. Reilly, C. M. Parker, J. M. Lonergan and T. J. Johnson, *Eur. J. Inorg. Chem.*, 2021, **2021**, 3277–3291.

8 C. Tamain, B. Arab-Chapelet, M. Rivenet, F. Abraham, R. Caraballo and S. Grandjean, *Inorg. Chem.*, 2013, **52**, 4941–4949.

9 J. P. Patterson and P. Parkes, in *The Nuclear Fuel Cycle*, ed. P. D. Wilson, Oxford Science Publications, Oxford, 1996, pp. 138–160.

10 B. Haidon, B. Arab-Chapelet, P. Roussel, T. Delahaye, M. Bertrand, S. Grandjean and M. Rivenet, in *Transactions of the American Nuclear Society*, 2017, vol. 116, pp. 78–81.

11 N. Vigier, S. Grandjean, B. Arab-Chapelet and F. Abraham, *J. Alloys Compd.*, 2007, **444–445**, 594–597.

12 B. Arab-Chapelet, P. M. Martin, S. Costenoble, T. Delahaye, A. C. Scheinost, S. Grandjean and F. Abraham, *Dalton Trans.*, 2016, **45**, 6909–6919.

13 R. M. Orr, H. E. Sims and R. J. Taylor, *J. Nucl. Mater.*, 2015, **465**, 756–773.

14 J. H. Christian, B. J. Foley, E. Ciprian, D. D. Dick, M. Said, J. Darvin, A. E. Hixon and E. Villa-Aleman, *J. Nucl. Mater.*, 2022, **562**, 153574.

15 L. E. Drabkina, A. I. Moskvin and A. D. Gel'man, *Zhurnal Neorg. Khimii*, 1958, **3**, 1934–1936.

16 A. D. Gel'man, L. E. Drabkina and A. I. Moskvin, *Zhurnal Neorg. Khimii*, 1958, **3**, 1546–1550.

17 R. Portanova, G. De Paoli, A. Bismondo and L. Magon, *Gazz. Chim. Ital.*, 1973, **10**, 691–697.

18 F. A. Zakharova, M. N. Orlova and N. N. Krot, *Radiokhimiya*, 1973, **15**, 786–789.

19 I. L. Jenkins, F. H. Moore and M. J. Waterman, *J. Inorg. Nucl. Chem.*, 1965, **27**, 77–80.

20 A. A. Bessonov, N. N. Krot, N. A. Budantseva and T. V Afonas'eva, *Radiochemistry*, 1996, **38**, 223–225.

21 M. K. Bhide, R. M. Kadam, Y. Babu, V. Natarajan and M. D. Sastry, *Chem. Phys. Lett.*, 2000, **332**, 98–104.

22 I. L. Jenkins and M. J. Waterman, *J. Inorg. Nucl. Chem.*, 1964, **26**, 131–137.

23 I. L. Jenkins, F. H. Moore and M. J. Waterman, *J. Inorg. Nucl. Chem.*, 1965, **27**, 81–87.

24 F. Abraham, B. Arab-Chapelet, M. Rivenet, C. Tamain and S. Grandjean, *Coord. Chem. Rev.*, 2014, **266**–**267**, 28–68.

25 N. N. Krot, A. A. Bessonov, I. A. Charushnikova and V. I. Makarenkov, *Radiochemistry*, 2007, **49**, 107–111.

26 Q. Liu, Q. Zhang, S. Yang, H. Zhu, Q. Liu and G. Tian, *Dalt. Trans.*, 2017, **46**, 13180–13187.

27 P. Di Bernardo, P. L. Zanonato, G. Tian, M. Tolazzi and L. Rao, *J. Chem. Soc., Dalton Trans.*, 2009, 4450–4457.

28 J. Havel, J. Soto-Guerrero and P. Lubal, *Polyhedron*, 2002, **21**, 1411–1420.

29 C. Görller-Walrand and K. Servaes, *Helv. Chim. Acta*, 2009, **92**, 2304–2312.

30 C. Manfredi, D. Ferri, E. Vasca, T. Caruso, V. Caruso, C. Fontanella, G. Palladino and S. Vero, *Ann. Chim.*, 2005, **95**, 313–324.

31 D. A. Skoog, F. J. Holler and C. S. R, *Principles of Instrumental Analysis*, Thomson Brooks/Cole, Belmont, California, 6th edn., 2007.

32 P. Atkins and J. de Paula, *Physical Chemistry: Thermodynamics, Structure, and Change*, Oxford University Press, Oxford, UK, 10th edn., 2014.

33 W. Hummel, G. Anderegg, L. Rao, I. Puigdomènech and O. Tochiyama, *Chemical Thermodynamics of Compounds and Complexes of U, Np, Pu, Am, Tc, Se, Ni and Zr with selected Organic Ligands*, OECD Nuclear Energy Agency, Issy-les-Moulineaux, France,

2005.

34 S. Okajima and D. T. Reed, *Radiochim. Acta*, 1993, **60**, 173–184.

35 I. Pashalidis, J. I. Kim, T. Ashida and I. Grenthe, *Radiochim. Acta*, 1995, **68**, 99–104.

36 S. D. Reilly and M. P. Neu, *Inorg. Chem.*, 2006, **45**, 1839–1846.

37 H.-R. Cho, E. C. Jung, K. K. Park, K. Song and J.-I. Yun, *Radiochim. Acta*, 2010, **98**, 555–561.

38 I. Grenthe, X. Gaona, A. Plyasunov, L. Rao, W. Runde, B. Grambow, R. J. M. Konings, A. L. Smith and E. E. Moore, in *Chemical Thermodynamics*, eds. M.-E. Ragoussi, J. S. Martinez and D. Costa, OECD, Boulogne-Billancourt (France), 2020, vol. 14.

39 Y. Jo, H. R. Cho and J. Il Yun, *Dalton Trans.*, 2020, **49**, 11605–11612.

40 D. T. Reed, S. Okajima and M. K. Richmann, *Stability of Plutonium(VI) in Selected WIPP Brines*, 1994, vol. 66–77.

41 W. Runde, S. D. Reilly and M. P. Neu, *Geochim. Cosmochim. Acta*, 1999, **63**, 3443–3449.

42 S. D. Reilly, W. Runde and M. P. Neu, *Geochim. Cosmochim. Acta*, 2007, **71**, 2672–2679.

43 H. Cho, E. C. Jung, M. H. Lee, K. K. Park, Y. J. Park, W. H. Kim and K. Y. Jee, in *Transactions of the Korean Nuclear Society Spring Meeting*, Jeju, Korea, 2007.

44 C. Xu, G. Tian, S. J. Teat, G. Liu and L. Rao, *Chem. - Eur. J.*, 2013, **19**, 16690–16698.

45 L. Xu, N. Pu, J. Yuan, P. Wei, X. Dong, Y. Wang, J. Chen and C. Xu, *New J. Chem.*, 2020, **44**, 3998–4003.

46 L. Rao, G. Tian, P. Di Bernardo and P. Zanonato, *Chem. - Eur. J.*, 2011, **17**, 10985–10993.

47 A. A. Bessonov and N. N. Krot, *Radiochemistry*, 2007, **49**, 571–574.

48 I. Puigdomenech, 2020. Medusa/Spana.

49 L. Ciavatta, *Ann. Chim.*, 1980, **70**, 551–562.

50 F. Crea, A. De Robertis, C. De Stefano and S. Sammartano, *Talanta*, 2007, **71**, 948–963.

51 A. Kirishima, Y. Onishi, N. Sato and O. Tochiyama, *Radiochim. Acta*, 2008, **96**, 581–589.

52 P. Di Bernardo, P. L. Zanonato, G. Tian, M. Tolazzi and L. Rao, *Dalton Trans.*, 2009, 4450–4457.

53 B. Brunel, V. Philippini, M. Mendes and J. Aupiais, *Radiochim. Acta*, 2015, **103**, 27–37.